NIH Public Access
Author Manuscript
Angew Chem Int Ed Engl. Author manuscript; available in PMC 2013 April 27.

Published in final edited form as:
Angew Chem Int Ed Engl. 2012 April 27; 51(18): 4358–4361. doi:10.1002/anie.201200997.

Significantly Improved Analytical Sensitivity of Lateral Flow Immunoassays by Thermal Contrast

Zhenpeng Qin,
Department of Mechanical Engineering, University of Minnesota, 111 Church St. SE, Minneapolis, MN 55455 (USA)

Warren C. W. Chan,
Institute of Biomaterials & Biomedical Engineering &Terrence, Donnelly Center for Cellular and Biomolecular Research

David R. Boulware,
Department of Medicine, Center for Infectious Disease and Microbiology Translational Research, University of Minnesota (USA)

Dr. Taner Akkin,
Department of Biomedical Engineering, University of Minnesota (USA)

Elissa K. Butler, and
Department of Medicine, Center for Infectious Disease and Microbiology Translational Research, University of Minnesota (USA)

John C. Bischof
Department of Mechanical Engineering, University of Minnesota, 111 Church St. SE, Minneapolis, MN 55455 (USA), Homepage: http://me.umn.edu/people/bischof.shtml. Department of Biomedical Engineering, University of Minnesota (USA). Department of Urology, University of Minnesota (USA)

John C. Bischof: bischof@umn.edu

Keywords

immunoassays; lateral flow; nanoparticles; sensors; thermal contrast

The ability to rapidly identify diseases enables prompt treatment and improves outcomes. This has increased the development and use of rapid point-of-care diagnostic devices capable of biomolecular detection in both high-income and resource-limited settings.[1] Lateral flow assays (LFAs) are inexpensive, simple, portable, and robust,[2] making LFAs commonplace in medicine, agriculture, and over-the-counter personal use such as for pregnancy testing. Although the analytical performance of some LFAs are comparable to laboratory based methods,[1a] the sensitivity of most LFAs is in the mM to μM range,[2–3] which is many folds less sensitive than other molecular techniques such as enzyme-linked immunoassays (ELISA). As a consequence, LFAs are not particularly useful for detection early in a disease course when there is low level of antigen. Due to the increasing need for highly sensitive molecular diagnostics, researchers have focused on developing microfluidics,[1a, 1b] biobar codes,[1c, 1d] and enzyme-based immunoassay technologies[4] technologies to fulfill the need since these technologies have nM to pM detection sensitivity

Correspondence to: John C. Bischof, bischof@umn.edu.

Supporting information for this article is available on the WWW under http://dx.doi.org/10.1002/anie.201200997.

NIH-PA Author Manuscript
NIH-PA Author Manuscript
NIH-PA Author Manuscript

NIH-PA Author Manuscript

NIH-PA Author Manuscript

NIH-PA Author Manuscript

for protein analysis and can potentially be miniaturized as handheld point-of-care diagnostic devices.[1c] These emerging technologies are still early in development and are not yet field-ready.

With LFAs, antibody-coated gold nanoparticles (GNPs) are moved within a nitrocellulose membrane through capillary action after the strip has been dipped in clinical specimen. When present, the target analyte binds to monoclonal antibody-coated GNPs. This bound complex stops wicking up the membrane when capture antibody on the membrane recognizes the antigen-antibody-GNP complex. This leads to accumulation of GNPs at the test line of the LFA, creating a visually positive test result, shown in Fig. 1. GNPs are traditionally used for LFAs because their size can be designed to easily migrate through the pores of the membrane; GNPs can be coated with antibodies easily; and GNPs have a high molar absorptivity of light producing deep color that is easily visualized. In this report, we show a low cost, creative solution to improve sensitivity of LFAs. Metallic nanoparticles generate heat upon optical stimulation.[5] This heat generation results from surface plasmons at the metal-dielectric interface during transition from an excited to ground state.[6] The amount of heat generated by GNPs can be described by the following equation:[5, 7]

$$Q = N \cdot Q_{nano} = N \cdot C_{abs} \cdot I \quad (1)$$

where the total heat generation (Q, W/m^3) is the combined contribution of single GNP (Q_{nano}, W), written as the product of GNPs concentration (N, nanoparticles - nps/m^3), GNP absorption cross section (C_{abs}, m^2), and laser intensity (I, W/m^2). As is now well known the optical,[8] thermal[9] and electrical[10] properties of materials change dramatically in the nanoscale. In particular, the enhanced photothermal signature of metal nanoparticles have been utilized for: thermal ablation of malignant tumors,[11] detecting circulating tumor cells,[12] photothermal molecule release[13] and gene transfection,[14] enhancing the therapeutic efficiency of chemotherapeutics,[15] and for tracking the transport of nanoparticles within cells.[16] Here, we determined whether thermal contrast could improve the analytical sensitivity of existing, commercial LFAs. Our results show a 32-fold improvement in analytical sensitivity using a FDA-approved cryptococcal antigen LFA with the potential to increase the sensitivity 10 000-fold by optimizing engineering design of the LFA substrate and nanoparticle.

First, we compared the thermal contrast versus visual contrast of GNPs in solution. A series of different concentrations of GNPs were prepared. 10 μL of the GNP solution was placed on a microscope slide. For visual analysis, a picture was taken by a digital camera and analyzed later with Image J. For thermal analysis, the GNP solution was irradiated with laser (0.5W, 532nm) and the temperature change was recorded by an infrared camera. Our results show that we can detect down to 2.5×10^9 nanoparticles/mL of GNPs using thermal contrast in comparison to 2.5×10^{11} nanoparticles/mL by visual contrast. This clearly demonstrates that thermal contrast for detection can improve the overall analytical sensitivity by 100-fold (Fig. 2B). We also compared thermal contrast of GNPs with standard optical density measurement using a standard micro-volume plate reader, the principle of which is widely used in microfluidic ELISA.[4] With the same sample volume (10μL), the thermal contrast displayed 50-fold improvement over the optical density measurement (Supplementary Fig. S1). Further improvement in thermal contrast sensitivity may be possible by using higher powered lasers and/or tuning the laser power for different concentrations of GNPs to extend the dynamic range of thermal contrast.

Next, we assessed the analytical performance of thermal contrast versus colorimetric detection (i.e. visual contrast) using FDA-approved LFAs for detecting cryptococcal antigen

NIH-PA Author Manuscript

NIH-PA Author Manuscript

NIH-PA Author Manuscript

(CrAg). Cryptococcosis is among the leading causes of death among all AIDS-related opportunistic infections and is the most common cause of meningitis in adults in Africa causing >500,000 deaths worldwide annually.[17] Cryptococcal meningitis (CM) is classically diagnosed by a combination of culture, India ink, or CrAg testing with semi-quantification by serial two-fold dilutions (i.e. CrAg titer, defined as the last positive test when performing two-fold serial dilutions). We compared by LFA serial 2-fold dilutions of a patient serum specimen with asymptomatic cryptococcal antigenemia,[18] positive at 1:32768 titer by latex agglutination (Immy, Inc.). Our results show that thermal contrast was indeed more sensitive than colorimetric visual detection on the LFA (Fig. 3A). Fig. 3B shows thermal contrast produced a 32-fold greater improvement in the analytical sensitivity than colorimetric detection with a log-linear slope up to an equivalent concentration of 1:1024 CrAg titer (S3 in Fig 3B) by latex agglutination (R^2 =0.98). Above this 1:1024 titer, there was a high dose "hook" effect with decreased visual intensity and a plateau of thermal intensity. This "effect" or "problem" can be overcome either by changing the dilution of the assay, or changing the engineering of the assay. We have further validated thermal contrast in 158 CSF samples with known CrAg titers from the 2006–2009 CM-cohort and including CSF specimens from patients with and without *Cryptococcus*[19], the correlation between the traditional (i.e. titer) and the new thermal contrast technique is R^2=0.88 (data not shown) without loss in specificity. In addition, the inter-assay precision of the assay can be improved by standardizing the size of these nanoparticles to decrease the coefficient of variance (Supplementary Fig S2). For comparison, the median CrAg titer observed in patients with cryptococcal meningitis is often 1:1024 to 1:2048.[20] However, there is a sub-acute onset over weeks to months with CrAg titers >1:8 in asymptomatic persons with subclinical disease predictive of later development of cryptococcal meningitis with 100% sensitivity and 96% specificity despite HIV therapy.[21] Serum CrAg screening and preemptive antifungal treatment in persons living with advanced AIDS aborts the clinical progression to symptomatic meningitis.[18] Non-invasive screening is possible with CrAg being detectable in urine, but urine has 22-fold lower CrAg concentration than blood.[22] Thus, improvement in LFA sensitivity by thermal contrast would enable non-invasive screening of asymptomatic persons with AIDS, and enable quantification of CrAg burden to stratify risk of future symptomatic disease.

Finally, we explored how to further improve the analytical sensitivity of LFAs. While spherical gold nanoparticles are conventionally used for LFAs, a new generation of nanoparticle structures has been synthesized with much higher absorption cross-sections than gold nanospheres. These new generation of nanoparticles include gold nanorods,[11d] nanoshells,[11a] and gold nanocubes.[11c] For instance, at the equivalent laser power and nanoparticle concentration, typical nanorods and nanoshells generate 4.6-fold and 36-fold more heat than gold nanospheres, respectively, shown in Fig 4A (with size specified in figure caption). To eliminate the particle size effect, the absorption cross section (C_{abs}) is normalized by particle volume (V) to give a better assessment of the heat generation capability. Using this normalization, gold nanorods are about one order of magnitude more efficient in heat generation than the gold nanospheres and nanoshells[5, 23] (Fig 4A inset). In addition, current LFAs (i.e. thin nitrocellulose membranes with thick backing material) absorb significant amounts of laser energy (at 532 nm) creating background heating or noise, shown in Fig. 4B. Thus, use of low absorbing (i.e. high transmitting or reflective) backing materials (e.g. glass shown in Fig. 2 and plastic used in microfluidic ELISA[4]) will allow the use of higher laser intensities (I). Combining higher absorbing nanoparticles and low absorbing LFA backing materials, further improvement in sensitivity will be expected. We should produce a 1000-fold increase in thermal contrast by increasing the power density by 100 times (i.e., increase in laser power from 0.01 to 1 W) and using a nanoparticle with a 10-fold increase in absorption (C_{abs}). Considering this and the 32 fold improvement already

NIH-PA Author Manuscript

NIH-PA Author Manuscript

NIH-PA Author Manuscript

shown in cryptococcal LFA (0.01 W laser and spherical GNP), a four order of magnitude improvement is possible.

Aside from the improvement in the analytical sensitivity, these LFAs can also be archived for future analysis. Unlike fluorescence detection, we did not observe any loss of signal through continuous excitation (Supplementary Fig S3). In fluorescence measurements, organic fluorophores experience photobleaching. In some colorimetric measurements, the dyes may lose their signal over time through photodestruction. When repeating thermal contrast readings at two weeks, the intra-assay reading is near identical (R^2=.99, data not shown). This could allow for processing point-of-care LFAs in the field and referral to a central lab to process for thermal contrast readings.

In conclusion, thermal contrast can be used on clinically-used LFAs to extend the analytical sensitivity by 32-fold. With further engineering modification (e.g. light source, nanoparticle absorption, and substrate) a 10, 000-fold improvement in sensitivity can be expected. This would bring the detection within the range of an ELISA assay. Due to the low cost and simple handheld nature of LFAs, this technology has applicability in resource-limited and non-laboratory environments with the “disposable LFAs with a reader” model[1a]. An inexpensive and portable thermal contrast reader could be built requiring only a low cost light-emitting diode (LED) and infrared temperature gun available over-the-counter or thermochromic ink that can be printed on paper.[24] Thus we conclude that the use of thermal contrast is a promising novel detection mode for improving the analytical sensitivity of biomolecular point-of-care diagnostics and expanding the use of LFAs.

Experimental Section

Thermal contrast imaging of GNP solution and LFAs

Titrated concentrations of GNP water solutions were prepared and 10μL of each solution was transferred to a glass slide as a drop. Laser beam from a CW Laser (532nm, Millennia Vs, Diode pumped) then irradiated the drop for 1 minute thereby inducing GNP heat generation. An infrared camera (FLIR ThermoVision™ A20) mounted at an angle above the sample measured temperature change remotely during laser irradiation. The maximum temperature change for each sample was determined from the thermal images and plotted. Similary, the test line of LFAs was irradiated by laser for 1 minute and recorded with an infrared camera. Complete experimental methods are available in the Supporting Information.

Acknowledgments

This work is supported partially by McKnight Professorship and Minnesota Futures Grant from the University of Minnesota, and NSF/CBET Grant #1066343(JCB). DRB is supported by the National Institute of Health, NIAID K23AI073192, and EB is supported by NIH NIAID U01AI089244. The authors thank Greg Huan and Vincent Blonigen for the help with the thermal contrast experiment, Neha Shah for the training of GNP synthesis, Robert Hafner and Pingyan Lei for the help with TEM imaging.

References

1. a Yager P, Edwards T, Fu E, Helton K, Nelson K, Tam MR, Weigl BH. Nature. 2006; 442:412–418. [PubMed: 16871209] b Martinez AW, Phillips ST, Whitesides GM, Carrilho E. Anal Chem. 2009; 82:3–10. [PubMed: 20000334] c Klostranec JM, Xiang Q, Farcas GA, Lee JA, Rhee A, Lafferty EI, Perrault SD, Kain KC, Chan WCW. Nano Lett. 2007; 7:2812–2818. [PubMed: 17705551] d Nam JM, Thaxton CS, Mirkin CA. Science. 2003; 301:1884–1886. [PubMed: 14512622]
2. Posthuma-Trumpie G, Korf J, van Amerongen A. Anal Bioanal Chem. 2009; 393:569–582. [PubMed: 18696055]

NIH-PA Author Manuscript NIH-PA Author Manuscript NIH-PA Author Manuscript

3. Liu J, Mazumdar D, Lu Y. Ang Chem Int Ed. 2006; 45:7955–7959.
4. Chin CD, Laksanasopin T, Cheung YK, Steinmiller D, Linder V, Parsa H, Wang J, Moore H, Rouse R, Umviligihozo G. Nat Med. 2011; 17:1015–1019. [PubMed: 21804541]
5. Govorov AO, Richardson HH. Nano Today. 2007; 2:30–38.
6. Maier, SA. Plasmonics: fundamentals and applications. Springer Verlag; 2007.
7. Qin Z, Bischof JC. Chem Soc Rev. 2012; 41:1191–1217. [PubMed: 21947414]
8. Kelly KL, Coronado E, Zhao LL, Schatz GC. J Phys Chem B. 2003; 107:668–677.
9. Shen S, Henry A, Tong J, Zheng R, Chen G. Nat Nanotechnol. 2010; 5:251–255. [PubMed: 20208547]
10. Dai H, Wong EW, Lieber CM. Science. 1996; 272:523.
11. a Hirsch LR, Stafford RJ, Bankson JA, Sershen SR, Rivera B, Price RE, Hazle JD, Halas NJ, West JL. Proc Natl Acad Sci USA. 2003; 100:13549–13554. [PubMed: 14597719] b von Maltzahn G, Park JH, Agrawal A, Bandaru NK, Das SK, Sailor MJ, Bhatia SN. Cancer Res. 2009; 69:3892–3900. [PubMed: 19366797] c Chen J, Wang D, Xi J, Au L, Siekkinen A, Warsen A, Li ZY, Zhang H, Xia Y, Li X. Nano Lett. 2007; 7:1318–1322. [PubMed: 17430005] d Dreaden EC, Alkilany AM, Huang X, Murphy CJ, El-Sayed MA. Chem Soc Rev. 2012
12. Galanzha E, Shashkov E, Kelly T, Kim J, Yang L, Zharov V. Nat Nanotechnol. 2009; 4:855–860. [PubMed: 19915570]
13. Bakhtiari ABS, Hsiao D, Jin G, Gates BD, Branda NR. Angew Chem Int Ed. 2009; 48:4166–4169.
14. a Braun GB, Pallaoro A, Wu G, Missirlis D, Zasadzinski JA, Tirrell M, Reich NO. ACS Nano. 2009; 3:2007–2015. [PubMed: 19527019] b Lu W, Zhang G, Zhang R, Flores LG, Huang Q, Gelovani JG, Li C. Cancer Res. 2010; 70:3177–3188. [PubMed: 20388791]
15. Hauck TS, Jennings TL, Yatsenko T, Kumaradas JC, Chan WCW. Adv Mater. 2008; 20:3832–3838.
16. Leduc C, Jung JM, Carney RR, Stellacci F, Lounis B. ACS Nano. 2011; 5:2587–2592. [PubMed: 21388224]
17. a Park BJ, Wannwmuehler KA, Marston BJ, Govender N, Pappas PG, Chiller TM. AIDS. 2009; 23:525–530. [PubMed: 19182676] b Jarvis JN, Meintjes G, Williams A, Brown Y, Crede T, Harrison TS. BMC Infect Dis. 2010; 10:67. [PubMed: 20230635]
18. Meya DB, Manabe YC, Castelnuovo B, Cook BA, Elbireer AM, Kambugu A, Kamya MR, Bohjanen PR, Boulware DR. Clin Infect Dis. 2010; 51:448–455. [PubMed: 20597693]
19. Boulware DR, Meya DB, Bergemann TL, Wiesner DL, Rhein J, Musubire A, Lee SJ, Kambugu A, Janoff EN, Bohjanen PR. PLoS Med. 2010; 7:e1000384. [PubMed: 21253011]
20. a Boulware DR, Bonham SC, Meya DB, Wiesner DL, Park GS, Kambugu A, Janoff EN, Bohjanen PR. J Infect Dis. 2010; 202:962–970. [PubMed: 20677939] b Bicanic T, Meintjes G, Rebe K, Williams A, Loyse A, Wood R, Hayes M, Jaffar S, Harrison T. J Acquir Immune Defic Syndr. 2009; 51:130–134. [PubMed: 19365271]
21. Jarvis JN, Lawn SD, Vogt M, Bangani N, Wood R, Harrison TS. Clin Infect Dis. 2009; 48:856–862. [PubMed: 19222372]
22. Jarvis JN, Percival A, Bauman S, Pelfrey J, Meintjes G, Williams GN, Longley N, Harrison TS, Kozel TR. Clin Infect Dis. 2011; 53:1019–1023. [PubMed: 21940419]
23. Jain P, Lee K, El-Sayed I, El-Sayed M. J Phys Chem B. 2006; 110:7238–7248. [PubMed: 16599493]
24. Siegel AC, Phillips ST, Wiley BJ, Whitesides GM. Lab Chip. 2009; 9:2775–2781. [PubMed: 19967113]

NIH-PA Author Manuscript
NIH-PA Author Manuscript
NIH-PA Author Manuscript

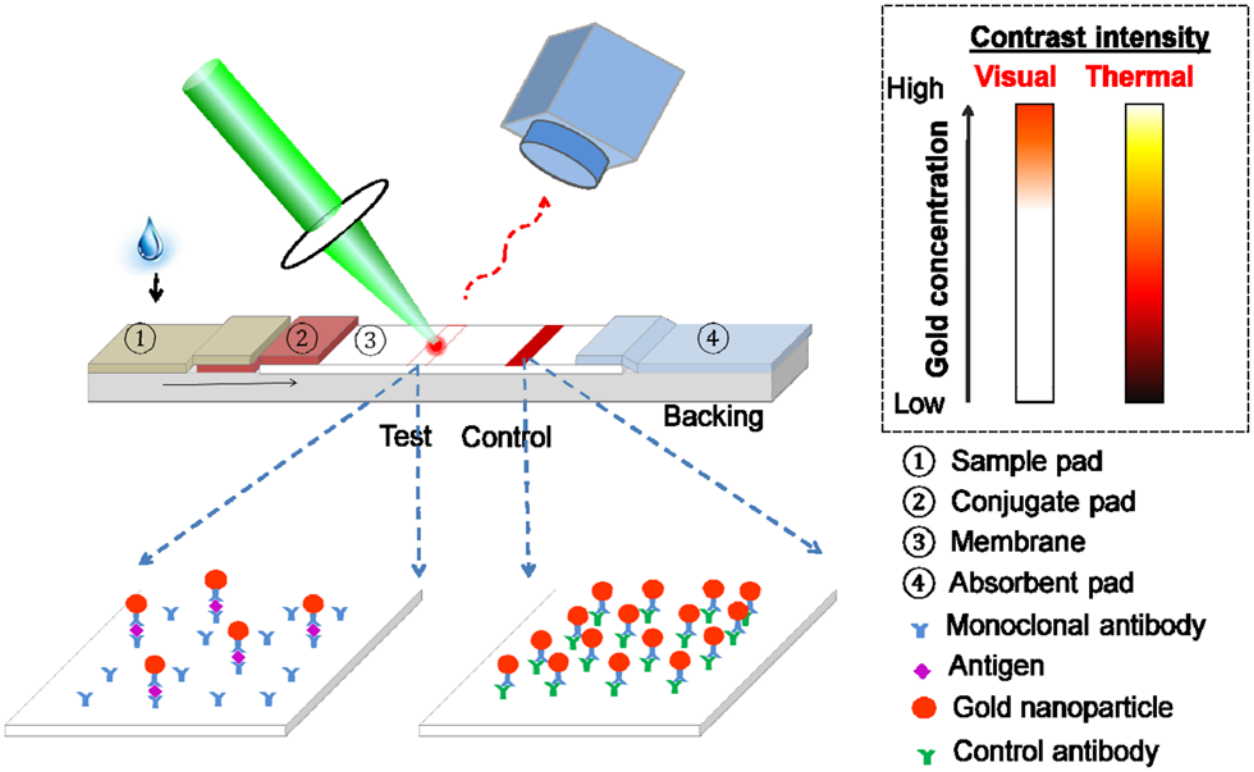

Figure 1.

Concept of thermal contrast for immunochromatographic lateral flow assays (LFAs). Monoclonal antibodies conjugated to gold nanoparticles (GNP) bind the target analyte. This GNP-antibody-antigen complex binds with monoclonal antibodies attached to the dipstick substrate, retaining the GNP in the test region and leading to visible color change (visual contrast) at the test band. Under low antigen conditions when there are insufficient bound GNPs for visual contrast, thermal contrast can detect the presence of GNPs in the test band (inset), with low-cost LED and infrared temp gun available over-the-counter. The control band ensures the success of the assay.

NIH-PA Author Manuscript

NIH-PA Author Manuscript

NIH-PA Author Manuscript

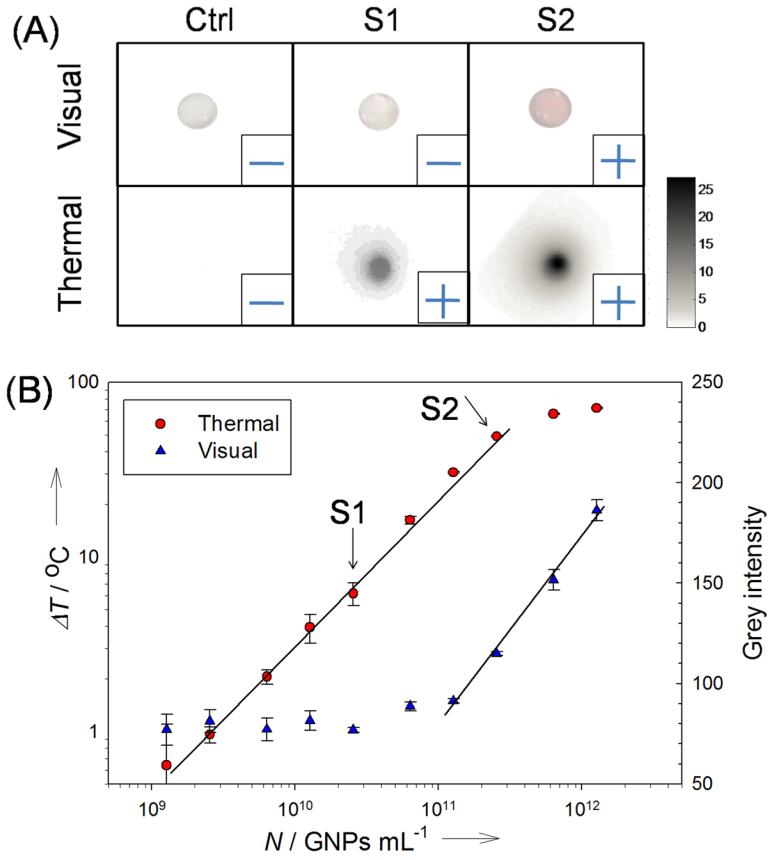

Figure 2.

Thermal contrast enhances the detection of gold nanoparticle (GNP) solution. (A) Examples of visual and thermal images of GNP solution and pure water.(B) Experimental demonstration showing 100-fold increase in the limit of detection with a CW laser (0.5W, 532nm wavelength). With higher laser power, lower concentrations of GNPs can be detected.

NIH-PA Author Manuscript

NIH-PA Author Manuscript

NIH-PA Author Manuscript

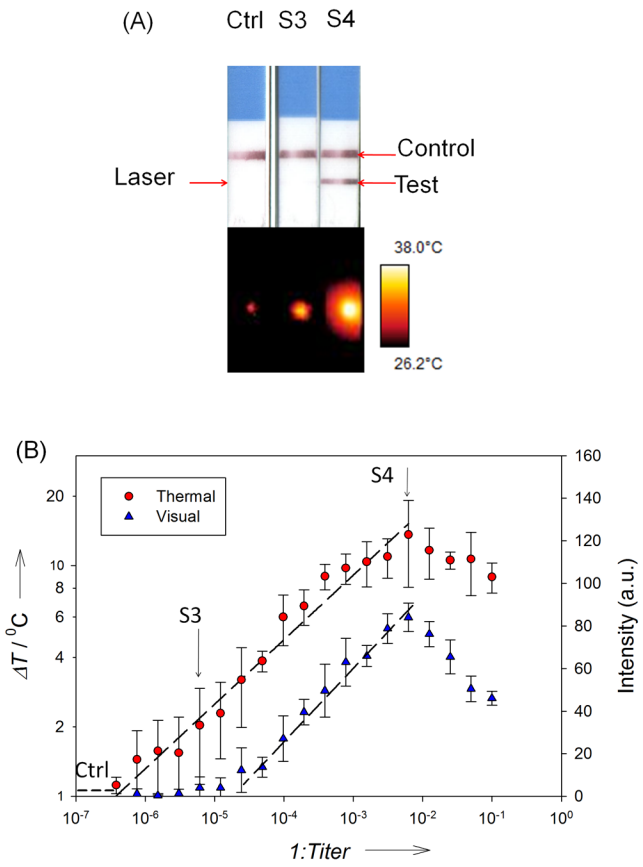

Figure 3.

Thermal contrast enhances the detection of existing immunochromatographic lateral flow assays for cryptococcal antigen (CrAg). (A) Examples of visual and thermal images of dipsticks used for CrAg diagnosis. (B) Quantitative measurement of the thermal and visual detection of LFA at 2-fold serial dilutions. Thermal contrast (laser power 0.01W) shows extended dynamic range vs. visual contrast. The drop of signal at high concentrations is due to the high dose hook effect inherent with the LFA. The dashed line shows background from the control samples.

NIH-PA Author Manuscript
NIH-PA Author Manuscript
NIH-PA Author Manuscript

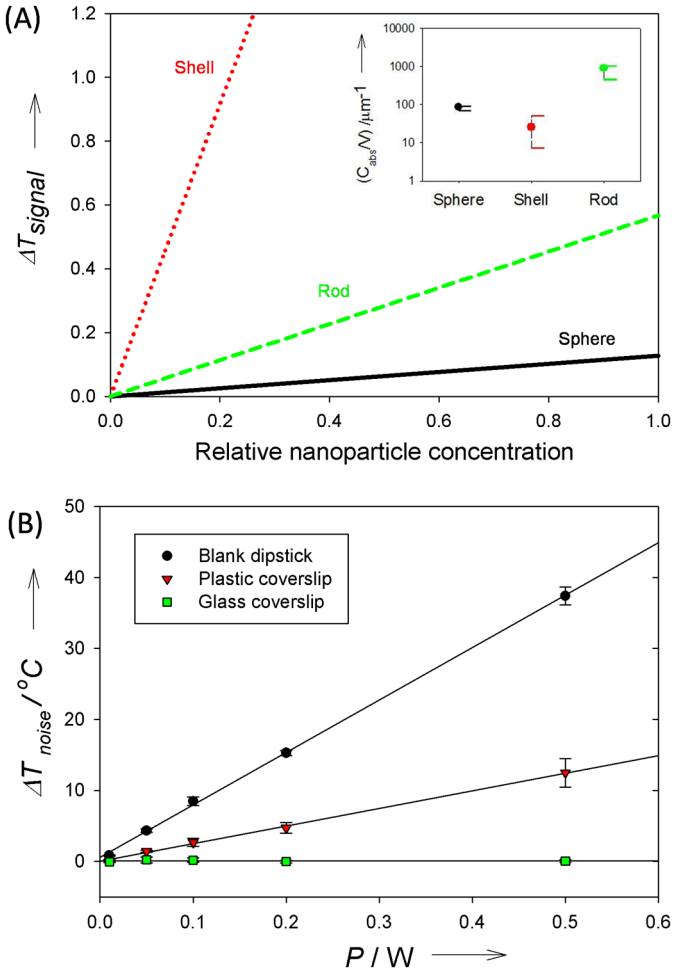

Figure 4.

Strategies to improve thermal contrast by several orders of magnitude.(A) Thermal contrast can be improved by increasing the absorption per nanoparticle. Particle parameters: sphere D=30nm, nanorod D=12.7nm by L=49.5nm, and nanoshell D_{core} = 120nm (silica), D_{shell}=150nm (gold). The thermal contrast (ΔT_{signal}) and nanoparticle concentrations are normalized. Inset shows the typical range of the absorption cross section per particle volume (C_{abs}/V) as calculated by Jain et al.[23]. The filled circles indicate the particular particles chosen for the plot. (B) Thermal contrast generated by different substrates with varying laser power (P). By reducing background absorption, this would: 1) increase the signal-to-noise ratio, and 2) allow the use of higher intensity laser excitation to increase the sensitivity and dynamic range of the thermal contrast measurement.